Radar Communication for Combating Mutual Interference of FMCW Radars

Canan Aydogdu, Nil Garcia, and Henk Wymeersch Department of Electrical Engineering, Chalmers University of Technology, Sweden e-mail: canan@chalmers.se

Abstract—Commercial automotive radars used today are based on frequency modulated continuous wave signals due to the simple and robust detection method and good accuracy. However, the increase in both the number of radars deployed per vehicle and the number of such vehicles leads to mutual interference among automotive radars, and cutting short future plans for autonomous driving and safety. We propose and analyze a radar communication (RadCom) approach to reduce or eliminate this mutual interference while simultaneously offering communication functionality. Our RadCom approach frequency division multiplexes radar and communication, where communication is built on a decentralized carrier sense multiple access protocol and is used to adjust the timing of radar transmissions. Our simulation results indicate that radar interference can be significantly reduced, at no cost in radar accuracy.

I. INTRODUCTION

Automotive radar is becoming an indispensable equipment in modern cars, for different functions including lane keeping, speed control and parking, especially due to its immunity to bad weather conditions [1]. Today, most automotive radar systems operate in 76-81 GHz [2], which provides a high range resolution on the order of centimeters [1] and the possibility of interference mitigation by locating the radars at different carrier frequencies [3], as a cost of performance. Likewise, vehicle-to-vehicle (V2V) communication is on the way to become a standard, having proven its value in dissemination of safety critical information [1], [4]. However, both technologies have some limitations related to increased penetration rates. Current automotive radar sensors are not controllable or able to coordinate with sensors from other vehicles. Hence, mutual radar interference becomes a problem, resulting in increased noise floor [5], [6], in turn resulting in reduced detection capability and ghost detections [7], see Fig. 1. Similarly, V2V communication systems, such as the IEEE 802.11p standard for dedicated short range communication (DSRC), are limited by the small allocated bandwidths, which in turn lead to low data throughput and inflexible medium access control (MAC). Omni-directional vehicular communication transmissions result in high interference with an increased number of vehicles [8]. This interference leads to packet losses, especially in emergency situations when many vehicles emit warning messages, in turn affecting system-wide safety.

Radar Communication (RadCom) is an approach to use radar hardware for communication purposes and can rely on the highly under-utilized frequency modulated continuous

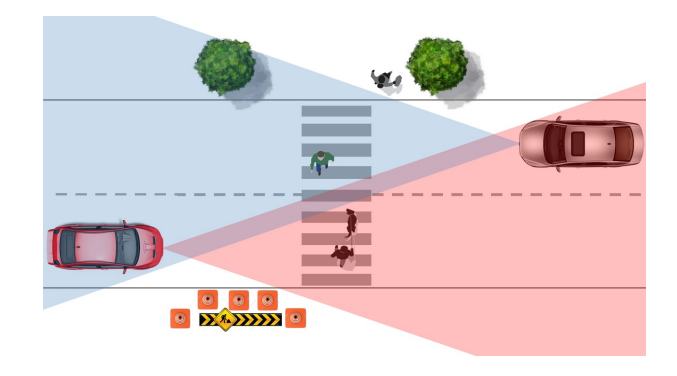


Fig. 1. Scenario with two vehicles in each other's field of view, leading to mutual interference.

wave (FMCW) radar bandwidth. This idea was first applied to a vehicular application, where radar and communication signals are transmitted between a vehicle and road side unit with a spread spectrum technique by two different chipping sequences [9]. Most of the other works consider orthogonal frequency division multiplexing (OFDM) for radar communications purpose [10]-[12]. OFDM is widely used in communication due to its high degree of flexibility, low receiver complexity, and high performance under different propagation conditions. The signal processing aspects of OFDM based RadCom is identified with its potential optimizations in [13]-[15] together with experimental test measurements to prove its applicability. An important challenge is that standard communication frequencies, such as the 5.9 GHz ISM band are generally unsuitable for radar, as the achieved accuracy and resolution is insufficient to meet automotive requirements [15]. In higher frequencies, a preliminary study for joint mmWave RadCom for vehicular environment in the 60GHz band [16]. used the IEEE 802.11ad preamble as a radar signal with standard WiFi receiver algorithms. It is shown that a reasonable range and velocity estimation accuracy (0.1m and 0.1m/s) is achieved by this technique. A similar study demonstrated how automotive sensor data relayed over DSRC is beneficial to the mmWave beam alignment, pointing out the possibility of adding mmWave communication functions on existing mmWave automotive radars in 76-81 GHz frequencies [17].

In this paper, we propose and analyze a novel RadCom approach for high-frequency FMCW radar, in which we repurpose a small part of the radar bandwidth to create an 802.11p-

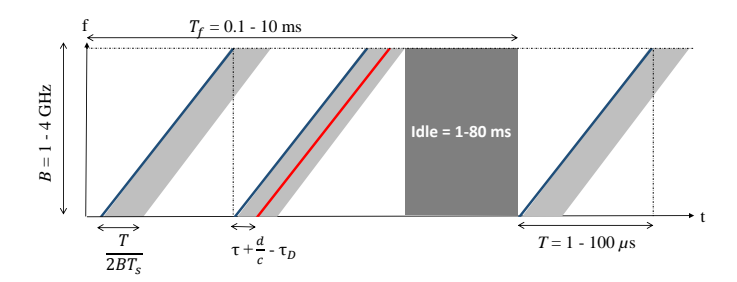


Fig. 2. FMCW modulation used in most automotive radar, with typical operating parameters. For a single radar, much of the time-frequency space is not utilized. The red line represents an interfering radar signal from another vehicle

like V2V connection. The V2V channel is controlled via a carrier sense multiple access (CSMA) protocol and is utilized to control the timing of radar signals. We have performed an in-depth simulation of the proposed concept for a two-vehicle scenario. We find that under realistic propagation conditions, RadCom can significantly reduce the radar interference, while no performance degradation in terms of radar accuracy.

II. SYSTEM MODEL

A. FMCW Transmitter

We consider a sequence of frequency modulated continuous waves, i.e., chirps, transmitted by an FMCW radar, of the form

$$s(t) = \sqrt{P_{tx}} \sum_{k=1}^{N} c(t - kT)$$

$$\tag{1}$$

where c(t) is a chirp of the form

$$c(t) = \exp(j2\pi(f_c + \frac{B}{T}t)t)$$
 (2)

 $P_{\rm tx}$ is the transmit power, B denotes the radar bandwidth (typically 1–4 GHz), f_c is the carrier frequency (77 GHz), T is the chirp duration, and N is the number of chirps per frame. The frame time T_f comprises NT plus the idle and processing time. Depending on the maximum detectable range (d_{\max}) and maximum detectable relative velocity (v_{max}) , plus range and velocity resolution of the FMCW automotive radar, T, T_f and N take typical values seen in Fig. 2. In Fig. 2 the signal format (frequency occupancy as a function of time) of a sawtooth FMCW signal is shown, where the blue line is the transmitted chirp, the grey band corresponds to the sampling bandwidth of the receiver and the red line is an interference received from a FMCW radar which started transmission with a τ time difference. After N successive chirps, there is a significant idle time used for processing the samples. Further, the white region indicates a large fraction of unused time-frequency resources.

B. FMCW Receiver

At the co-located receiver, the backscattered signal is processed. The radar receiver comprises of the following blocks [18]: a mixer, an analog-to-digital convertor (ADC), and a digital processor. The mixer multiplies the received signal

with a copy of the transmitted chirp. After low-pass filtering the resulting intermediate frequency (IF) signal, the mixer will output a signal with multiple harmonics at frequencies proportional to the time difference between the transmitted chirp and the received chirps. The output of the mixer is then sampled by the ADC, with sampling interval T_s , and passed to the digital processor which will detect and estimate the frequencies. The ADC bandwidth $1/(2T_s)$ is generally on the order of 10–50 MHz and is thus much smaller than B. Considering a single target at distance d, the sampled back-scatter signal, sample n or chirp k is of the form [1]

$$r_n^{(k)} = \sqrt{\gamma P_{\text{tx}} d^{-4}} \exp\left(j2\pi \frac{B(2d/c - 2\tau_D)}{T} nT_s\right) + w_n^{(k)}$$
(3)

where $\gamma = G_{\rm tx}G_{\rm rx}\sigma\lambda^2/(4\pi)^3$, for target radar cross section (RCS) σ , transmitter and receiver antenna gains $G_{\rm tx}$ and $G_{\rm rx}$, Doppler time shift $\tau_D = Tvf_c/(Bc)$, in which c denotes the speed of light, v is the relative velocity between vehicles (note that a positive v corresponds to approaching vehicles and a positive Doppler shift, which leads to a decreased time difference between the transmitted and reflected radar signal), $w_n^{(k)}$ is additive white Gaussian noise (AWGN) with variance N_0 . A common approach to frequency retrieval in FMCW radar is to compute the fast Fourier transform (FFT) of the signal, average the signal through multiple chirp periods for enhanced SNR, and detect the peaks in the frequency-domain.

C. Goal

Our aim is to study the performance of the receiver when the target is itself a vehicle with FMCW radar. We propose an FMCW-based RadCom system and investigate how the probability of mutual interference, the probability of false alarm and the ranging error are effected by the proposed scheme.

III. RADAR INTERFERENCE ANALYSIS

In this section, we describe the interference model and calculate the conditions under which interference exists, both for a single link and for a network.

A. Interference Model

Consider the scenario in Fig. 1. Two cars with front-end FMCW radars facing each other approach a road-crossing where pedestrians are present. Both radars are FMCW based and use the same frequency band. If the interfering radar is located at distance d and has a relative delay τ between the ego vehicle transmission and the interfering vehicle transmission, then the received signal at the ego radar becomes

$$\tilde{r}_{n}^{(k)} = \begin{cases} r_{n}^{(k)} & \tau \notin V \\ r_{n}^{(k)} + \sqrt{\tilde{\gamma}P_{\text{tx}}d^{-2}} \exp\left(j2\pi \frac{B(\tau + d/c - \tau_{D})}{T}nT_{s}\right) & \tau \in V \end{cases}$$

where $\tilde{\gamma} = G_{\rm tx} G_{\rm rx} \lambda^2/(4\pi)^2$ and V is the so-called *vulnerable* period, defined as the time interval during which received signals from facing radars causes mutual interference. The

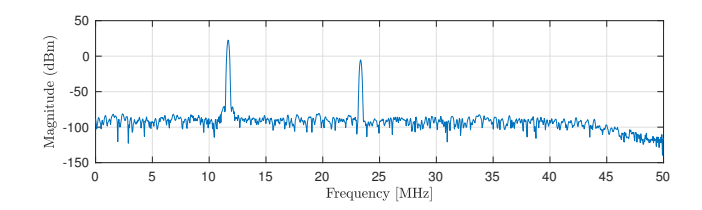


Fig. 3. FFT of received signal, with a interfering vehicle target at $d=70\,$ and a ghost target at 35 m.

interfering signal transmitted by a time difference of τ is received at the ego radar at $\tau + d/c - \tau_D$ as illustrated in Fig. 2. We note that interference has a factor d^{-2} while the useful signal has a factor d^{-4} , leading to an interference that is much stronger than the useful signal. Fig. 3 shows an example of such a received FMCW signal, for vehicle target at distance 70 m from the radar, with $\tau = 0$, which in this case is in the vulnerable period. The target is observed at 23.33 MHz, whereas the strong interference is observed at 11.67 MHz, corresponding to 35 m. The vulnerable period will now be determined.

B. Single Link Interference Condition

Let us assume the ego vehicle starts an FMCW transmission at time t=0. Suppose the interfering vehicle starts a transmission at time $t=\tau$. We will now determine the vulnerable period for different conditions.

• Without Doppler: The interfering transmission arrives at the ego vehicle at time $t' = \tau + d/c$. Interference will occur when $t' \in [0, T/(2BT_s)]$. Hence, the vulnerable period for the ego vehicle corresponds to all transmission times t' of other vehicles for which

$$\tau \in V = \left[-d_{\text{max}}/c, T/(2BT_s) \right] \tag{5}$$

where d_{max} is the maximum detectable radar range and is related to chirp parameters by $d_{\text{max}} = cT/(4BT_s = [19]$.

• With Doppler: If we further account for Doppler, the vulnerable period for a transmission at time t=0 is then given by

$$V = \left[-\frac{d_{\text{max}}}{c} - \frac{T v_{\text{max}} f_c}{B c}, \frac{T}{2BT_s} + \frac{T v_{\text{max}} f_c}{B c} \right]$$
 (6)

where $v_{\rm max}$ is the maximum detectable relative velocity (approaching or receding) and is given by $v_{\rm max} = c/(4f_cT)$ [19].

• With imperfect low-pass filtering: Reception of negative edge frequencies of the imperfect low-pass filtering at the ADC also cause mutual interference, especially for smaller d when the interference power is so high that it still resides after low-pass filtering. This leads to extension of the vulnerable period to

$$V = \left[-\frac{T}{BT_s} - \frac{d_{\text{max}}}{c} - \frac{T v_{\text{max}} f_c}{B c}, \frac{T}{2BT_s} + \frac{T v_{\text{max}} f_c}{B c} \right].$$
(7)

From this, it follows that the probability of interference for a single chirp is

$$P_{\text{int}}^{(c)} \approx \frac{3}{2BT_c} + \frac{d_{\text{max}}}{cT} + 2\frac{v_{\text{max}}f_c}{cB} \tag{8}$$

$$\approx \frac{7}{4BT_s} + \frac{1}{2BT} \approx \frac{2}{BT_s} \tag{9}$$

since $T_s \ll T$.

We can further account for the idle time as follows: the interfering vehicle transmits during a fraction NT/T_f of the frame period, so that the probability of interference is reduced to

$$P_{\text{int}}^{(f)} = \frac{P_{\text{int}}^{(c)} NT}{T_f} \tag{10}$$

Remark 1. Note that we have not accounted for reflections or additional targets in the environment. Such targets could also lead to interference. For that reason the vulnerable period could further be extended, following the same procedure as above.

C. Network Interference Condition

For a network of vehicles, we first study a star topology around the ego vehicle. When there are M interfering vehicles, the probability of interference is $P_{\text{int}}^{(M)} = 1 - (1 - P_{\text{int}}^{(f)})^M$. For a more general topology with M vehicles, let G be a directed radar graph with $G = (\mathcal{V}, \mathcal{E})$, where each vertex corresponds to a radar $r_i \in \mathcal{V}$ and each edge e_{ij} means that radar i is the field of view of radar j. The average probability of interference is then given by

$$-T/\bar{P} = \frac{1}{|\mathcal{V}|} \sum_{r_i \in \mathcal{V}} P_{\text{int}}^{(M_i)} \tag{11}$$

where M_i denotes the number of edges into r_i .

D. Performance under Radar Interference

So-far we have only treated the probability of radar interference. When there is interference, we know from (4) that the interfering signal is generally stronger than the useful signal. This affects radar performance in a number of ways: it leads to ghost targets and an increase of the noise floor. Relevant performance metrics are thus the probability of detection, the probability of false alarm, and the ranging accuracy of the targets. These metrics will be analyzed in detail in Section V.

IV. RADCOM FOR INTERFERENCE REDUCTION

An FMCW-based-RadCom system is composed of three parts for sharing the wireless channel resource:

- Multiplexing scheme for sharing among radar and communication,
- Radar MAC scheme (rMAC) for coordination of radar sensing among different vehicles and
- 3) Communication MAC scheme (cMAC) for sharing among different vehicles.

In this study, we propose a RadCom scheme, where radar and communication are frequency division multiplexed (FDM) [20] with a time division multiple access for radar signals

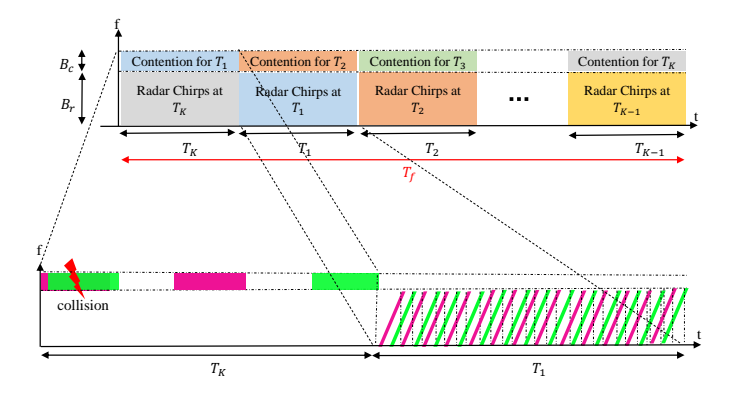


Fig. 4. RadCom scheme: FDM / rTDMA / cCSMA. The time division multiplexed radar starting times for slot T_i are determined by p-peristent CSMA contentions that take place in slot T_{i-1} .

(rTDMA), and a p-persistent CSMA for communication signals (cCSMA). Fig. 4 illustrates the division of the frequency and time domains for the proposed FDM/rTDMA/cCSMA based RadCom system.

A. Multiplexing

Although multiplexing can be avoided by considering a joint waveform for communication and radar, such an approach is not suitable for automotive applications due to the limited ADC capabilities, which do not support full-band communication (e.g., OFDM) and modulating FMCW chirps would lead to extremely low data rates. Hence, we divide up the bandwidth B into a radar band B_r and a communication bandwidth B_c , for which $B_r + B_c \leq B$ and $B_c < 1/2T_s$, in order to be able to reuse the radar ADC.

B. Radar MAC

Current FMCW automotive radar operation is limited by the ADC sampling rate, which can be turned into an advantage to collocate different radar signal sweeps in time. In other words, FMCW radars of different vehicles use the channel in a TDMA manner without causing mutual interference among each other if the time difference of starting time of chirps are adjusted such that these chirps are not received during the vulnerable period. In particular, as explained in Section III-B, an interfering radar should avoid transmissions during the vulnerable period V.

As illustrated in Fig. 4, one radar frame duration is divided into time slots T_i of length (N+1)T, which corresponds to the duration for sending N chirps plus one idle chirp time. This slotted time is set to provide non-overlapping chirp sequences and thereby maximize the number of vehicles with no mutual interference in the RadCom system, defined by $M_{\rm max}$. Denoting the duration of the vulnerable period by |V|, for the proposed rTDMA, at most $\lfloor T/|V| \rfloor$ different vehicle radars can coexist in a slot T_i and the maximum number of time slots per frame is $K = \lfloor T_f/(N+1)T \rfloor$, which limit $M_{\rm max}$ under perfect communication by

$$M_{\text{max}} \le K |T/|V|| \tag{12}$$

Vehicles are assumed to synchronize their clocks using the global navigation system sensors. Each vehicle selects a random frame starting time from a set of possible times with disjoint vulnerable periods V.

C. Communication

V2V vehicular communication is used to coordinate the starting time of radar frames. Communication is assumed to take place in a separate frequency channel of bandwidth B_c by p-persistent CSMA. The communication channel is also divided to time slots T_i as illustrated in Fig. 4. Contentions among vehicles are resolved the time slot T_{i-1} , where each a communication packet (a fixed number of bytes with a fixed modulation format) is broadcast advertising the starting time of the first chirp in the next time slot T_i . Other vehicles receiving this packet adjust their starting time by selecting a frame starting time for radar transmissions (rTDMA) according to the vulnerable period V. All vehicles communicating in slot T_{i-1} agree upon a radar frame starting time to be affective in slot T_i . Since communication links are not necessarily symmetric due to the directed RadCom transmissions, a best effort approach with no acknowledgements is used. During the communication slot T_i , time is further assumed to be subdivided into slots equal to the communication packet duration for p-persistent CSMA operations employed, such as carrier sensing and backoff. Exponential backoff is employed in the proposed RadCom system.

V. PERFORMANCE EVALUATION AND RESULTS

The performance of an FMCW receiver when the target is itself a vehicle with FMCW radar is investigated. And a comparison is made by the proposed FMCW-based RadCom system in terms of the probability of false alarm and the ranging error. The probability of mutual interference and the necessary time to resolve contention for multiple vehicles are evaluated.

A. Simulation Parameters

The simulation parameters are summarized in Table I. Two facing vehicles are assumed to have radars with the same properties. Radar is FMCW with sawtooth waveform. The chirp sequence is designed so as to meet the maximum detectable relative velocity $v_{\rm max}=140$ km/h, the maximum detectable range $d_{\rm max}=150$ m, velocity resolution smaller than 1 m/s and range resolution of 15 cm. Radar front-endhardware component parameters are taken as in [18]. The mean value for the radar cross section of a car is taken as 20 m² [18], [21]. At the signal processing stage, coherent pulse integration is applied. Moreover, a Blackman-Harris window to reduce the height of the sidelobes is applied before the FFT module. Finally, greatest of cell averaging constant false alarm rate (GoCA-CFAR) thresholding with 50 training cells with 2 guard cells is used for radar detection. The vulnerable duration is computed to be $|V| = 3.5 \mu s$ (7), leading to maximum 5 concurrent radar transmissions per T_i , resulting with $M_{\text{max}} = 50$ maximum number of vehicles supported by the proposed RadCom system (12).

TABLE I SIMULATION PARAMETERS.

	Parameter	Value
Radar	Chirp duration (T)	20 μs
	Frame duration (T_f)	20 ms
	Time slots per frame (K)	10
	Radar bandwidth	0.96 GHz-1 GHz
	$d_{ m max}$	150 m
	$v_{ m max}$	140 km/h
	$P_{ m tx}$	1 Watt
	N	99
	f_c	77
	T_s	0.01 μs
	Chebyshev low-pass filter order	13
	Thermal noise temperature	290 K
	Receiver's noise figure	4.5 dB
Comm.	Communication bandwidth B_c	20 MHz,40 MHz
	Packet size	600 Bytes
	Modulation	16-QAM
	MAC	p-persistent CSMA with $p = 1/M$
	Maximum contention window	6

B. Results

We will first consider probability of the radar interference for a multi-vehicle scenario, and then evaluate the RadCom performance in terms of delay to resolve contentions. Finally, we present in-depth results for two vehicles, with an without RadCom.

- 1) Radar Interference: The average probability of interference, \bar{P} , for varying separation distance between vehicles on a lane and different number of lanes is given by Fig. 5 for $B_c=20$ MHz. The average probability of interference increases by lower vehicle separation and higher number of lanes, i.e., increased density of vehicles. We conclude that for dense multi-lane traffic, radar interference is a grave concern, despite the low duty cycle.
- 2) Communication Delay: We denote the time to resolve contention among connected M vehicles by $t_{\rm final}$. The vehicles apply p-persistent CSMA with p=1/M (in practice the vehicles would need to estimate the number of neighbors). Based on 10,000 Monte Carlo runs, Fig. 6 shows the average, minimum, and maximum value of $t_{\rm final}$ as a function of M for $B_c=20$ MHz. We assume that all M stations initiate transmission attempts during the time slot T_1 . We observe that the contention time for $M_{\rm max}=50$ vehicles meets this requirement on the average, but the contention time can last up to 50 ms, which means that the coordination of some vehicles may last longer than a radar frame time. For $B_c=40$ MHz the results for $t_{\rm final}$ halves favoring of the proposed RadCom scheme.
- 3) Radar Interference with RadCom: The performance of RadCom is evaluated for the communication bandwidths $B_c \in \{20, 40\}$ MHz. The distance between two vehicles (d) and the time difference between starting times of chirps (τ) are varied. The performance of radar only and RadCom schemes are compared in terms of probability of false alarm (P_f) and ranging error based on 100 Monte Carlo simulations. Fig. 7 shows the probability of false alarm without RadCom for

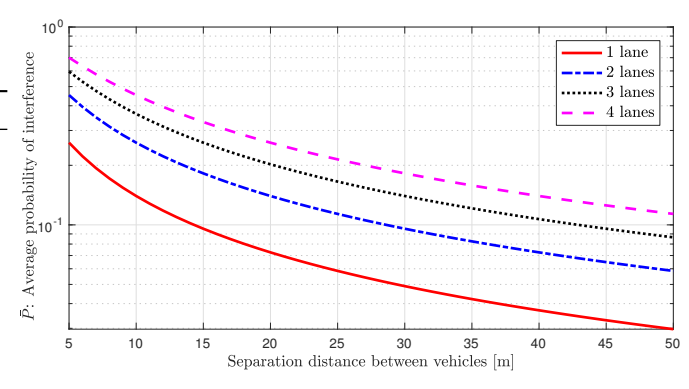


Fig. 5. Average probability of interference for varying vehicle separation distance and different number of lanes for $B_c=20~{\rm MHz}.$

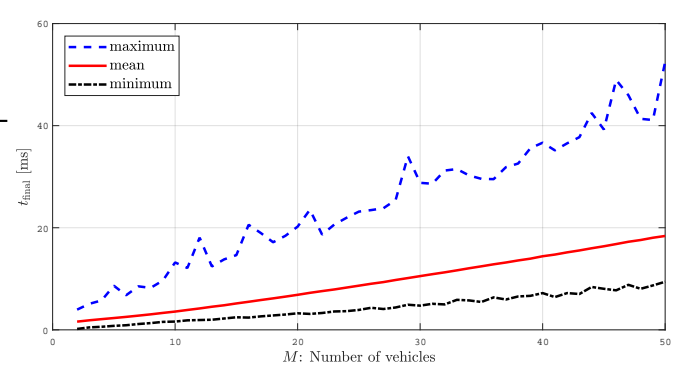


Fig. 6. Time necessary to resolve communication contention among M vehicles for $B_c=20$ MHz.

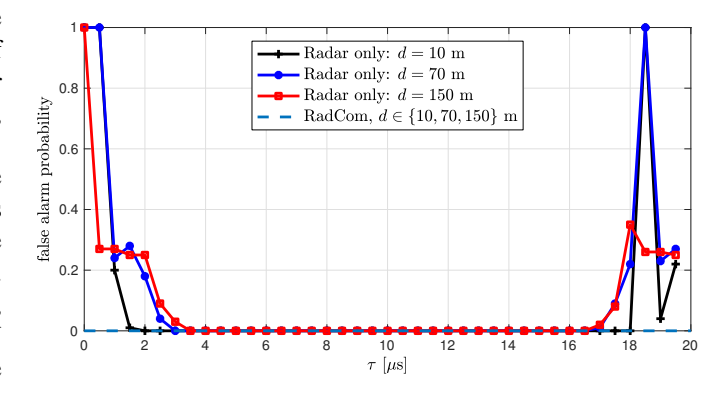


Fig. 7. Comparison of probability of false alarm between radar and RadCom with $B_{\rm c}=20$ MHz.

 $B_c=20$ MHz for varying τ and three different d values. The transmissions during the vulnerable period V is observed to result with interference for especially $\tau < T/(2BT_s) = 1 \, \mu s$ and $\tau = 18 - 20 \, \mu s$, due to the imperfect low-pass filtering, described in (7). With RadCom, the false alarm probability was rediced to zero for all τ and d.

Fig. 8 shows the ranging error performance with and without RadCom. Simulations taken over varying τ and d, show that the ranging error is independent of τ and below 9 cm for all cases. We note that in the considered scenario, we were not limited by the noise, so that the ranging error is a deterministic

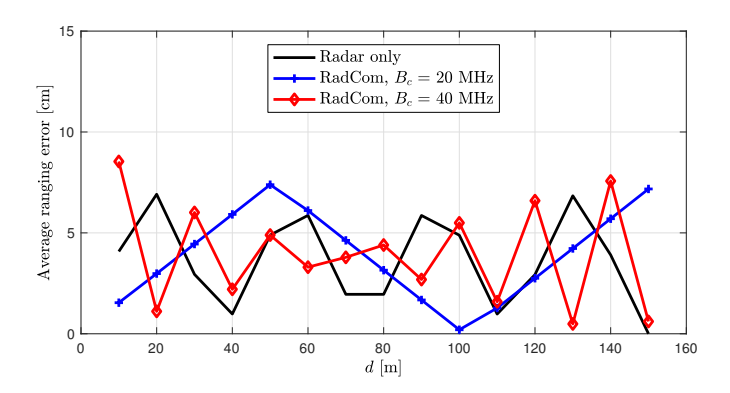


Fig. 8. Comparison of ranging error without and with RadCom of $B_c=20\,$ MHz and $B_c=40\,$ MHz.

function of τ , d, and the receiver-side signal processing. While RadCom in theory leads to an accuracy reduction due to reduced bandwidth, this effect can be neglected.

VI. CONCLUSION

We have evaluated a RadCom approach building on a combination of FDM, TDMA for radar, and CSMA for communication. The approach exploits the low utilization of time and frequency of a typical radar, as well as the limited impact of a small bandwidth loss on the radar performance. We have performed an interference analysis at both the link and network level and found that with higher penetration, interference is prevalent. With our proposed approach, we are able to mitigate interference by shifting radar transmissions in time. Performance in terms of false alarms, missed detections, and ranging accuracy are reported, based on high-fidelity simulations. Future work will consider larger-scale scenarios as well as the interference from multipath.

ACKNOWLEDGMENT

This work was supported, in part, by Marie Curie Individual Fellowships (H2020-MSCA-IF-2016), Grant 745706 (GreenLoc), and a SEED grant from Electrical Engineering Department of Chalmers University of Technology.

REFERENCES

- [1] S. M. Patole, M. Torlak, D. Wang, and M. Ali, "Automotive radars: A review of signal processing techniques," *IEEE Signal Processing Magazine*, vol. 34, no. 2, pp. 22–35, 2017.
- [2] J. Hasch, E. Topak, R. Schnabel, T. Zwick, R. Weigel, and C. Wald-schmidt, "Millimeter-wave technology for automotive radar sensors in the 77 GHz frequency band," *IEEE Transactions on Microwave Theory and Techniques*, vol. 60, no. 3, pp. 845–860, March 2012.
- [3] T. Schipper, M. Harter, L. Zwirello, T. Mahler, and T. Zwick, "Systematic approach to investigate and counteract interference-effects in automotive radars," in *Radar Conference (EuRAD)*, 2012 9th European. IEEE, 2012, pp. 190–193.
- [4] L. Kong, M. K. Khan, F. Wu, G. Chen, and P. Zeng, "Millimeter-wave wireless communications for IoT-cloud supported autonomous vehicles: Overview, design, and challenges," *IEEE Communications Magazine*, vol. 55, no. 1, pp. 62–68, January 2017.
- [5] M. Goppelt, H.-L. Blöcher, and W. Menzel, "Analytical investigation of mutual interference between automotive FMCW radar sensors," in *Microwave Conference (GeMIC)*, 2011 German. IEEE, 2011, pp. 1–4.

- [6] A. Bourdoux, K. Parashar, and M. Bauduin, "Phenomenology of mutual interference of FMCW and PMCW automotive radars," in 2017 IEEE Radar Conference (RadarConf), May 2017, pp. 1709–1714.
- [7] I. M. Kunert, "Project final report, MOSARIM: More safety for all by radar interference mitigation," 2012. [Online]. Available: http://cordis.europa.eu/docs/projects/cnect/1/248231/ 080/deliverables/001-D611finalreportfinal.pdf
- [8] A. Rostami, B. Cheng, G. Bansal, K. Sjöberg, M. Gruteser, and J. B. Kenney, "Stability challenges and enhancements for vehicular channel congestion control approaches," *IEEE Transactions on Intelligent Transportation Systems*, vol. 17, no. 10, pp. 2935–2948, 2016.
- [9] M. Takeda, T. Terada, and R. Kohno, "Spread spectrum joint communication and ranging system using interference cancellation between a roadside and a vehicle," in *Vehicular Technology Conference*, 1998. VTC 98. 48th IEEE, vol. 3, May 1998, pp. 1935–1939 vol.3.
- [10] B. J. Donnet and I. D. Longstaff, "Combining MIMO radar with OFDM communications," in 2006 European Radar Conference, Sept 2006, pp. 37–40.
- [11] D. Garmatyuk, J. Schuerger, and K. Kauffman, "Multifunctional software-defined radar sensor and data communication system," *IEEE Sensors Journal*, vol. 11, no. 1, pp. 99–106, Jan 2011.
- [12] C. Sturm and W. Wiesbeck, "Waveform design and signal processing aspects for fusion of wireless communications and radar sensing," *Proceedings of the IEEE*, vol. 99, no. 7, pp. 1236–1259, July 2011.
- [13] P. Falcone, F. Colone, C. Bongioanni, and P. Lombardo, "Experimental results for OFDM wifi-based passive bistatic radar," in 2010 IEEE Radar Conference, May 2010, pp. 516–521.
- [14] C. Sturm, T. Zwick, W. Wiesbeck, and M. Braun, "Performance verification of symbol-based OFDM radar processing," in 2010 IEEE Radar Conference, May 2010, pp. 60–63.
- [15] L. Reichardt, C. Sturm, F. Grunhaupt, and T. Zwick, "Demonstrating the use of the IEEE 802.11p car-to-car communication standard for automotive radar," in 2012 6th European Conference on Antennas and Propagation (EUCAP), March 2012, pp. 1576–1580.
- [16] P. Kumari, N. Gonzalez-Prelcic, and R. W. Heath, "Investigating the IEEE 802.11ad standard for millimeter wave automotive radar," in 2015 IEEE 82nd Vehicular Technology Conference (VTC2015-Fall), Sept 2015, pp. 1–5.
- [17] J. Choi, V. Va, N. Gonzalez-Prelcic, R. Daniels, C. R. Bhat, and R. W. Heath, "Millimeter-wave vehicular communication to support massive automotive sensing," *IEEE Communications Magazine*, vol. 54, no. 12, pp. 160–167, December 2016.
- [18] C. Karnfelt, A. Paden, A. Bazzi, G. E. H. Shhade, M. Abbas, and T. Chonavel, "77 GHz ACC radar simulation platform," in 2009 9th International Conference on Intelligent Transport Systems Telecommunications, (ITST), Oct 2009, pp. 209–214.
- [19] M. I. Skolnik, Radar Handbook, 3rd ed. New York: McGraw-Hill Education, 2008.
- [20] H. Hellsten and P. Dammert, "Short range radar cohabitation: Extension to integrated communication," Saab Surveillance Report, 2017.
- [21] S. Lee, S. Kang, S. C. Kim, and J. E. Lee, "Radar cross section measurement with 77 GHz automotive FMCW radar," in 2016 IEEE 27th Annual International Symposium on Personal, Indoor, and Mobile Radio Communications (PIMRC), Sept 2016, pp. 1–6.